VOL. 11, NO. 11, JUNE 2016 ISSN 1819-6608
ARPN Journal of Engineering and Applied Sciences

www.arpnjournals.com

NUMERICAL ESTIMATION OF MECHANICAL PROPERTIES OF STRUCTURAL STEEL COMPONENTS AT ELEVATED TEMPERATURES

Youngjin Seo[1] and Woosuk Kim[2]
[1]Department of Mechanical Engineering, Kumoh National Institute of Technology, Daehak-ro, Gumi, Korea
[2]School of Architecture, Kumoh National Institute of Technology, Daehak-ro, Gumi, Korea
E-Mail: wkim@kumoh.ac.kr

ABSTRACT

The 2001 World Trade Center attack has led to greater interest in the complexities of cities and the concentration of buildings. Hence, toward maximizing the protection of citizens and property in advanced high-capacity structures, we evaluated the use of performance-based design methods as an alternative to prescription-based methods, to determine the physical properties of steel structures under the effects of fire-induced high temperatures. We developed a model for evaluating the effects of fire on the engineering properties of such structures, and also considered the material properties of steel structures exposed to ISO 834 fire conditions. The heat conduction was analyzed by a finite element method (FEM). Based on the output data on the elements of the steel members, a heat elastoplastic creep analysis program was used to analyze the resistance capacity of the steel structure with respect to the load, size of the section, and length of the member.

Keywords: performance-based design, steel structures, heat conduction, elastoplastic creep analysis, fire resistance.

INTRODUCTION

Steel frame structures are extensively used in the construction of highrise buildings in major cities of the world owing to the advantages of a shortened construction time and reduced weight compared to the use of concrete. However, steel has less fire resistance than concrete, and the strength and stiffness of a steel frame under temporary loads due to fire-induced thermal conduction are significantly lower than those of a concrete structure. Hence, in the event of fire in a steel building, the structural members may be seriously damaged, with the possibility of total collapse during a flashover or decay phase.

To enhance safety, most domestic buildings are designed and constructed using fire resistant structures developed by various generalized prescriptive standards. We believe, however, that modern standards need to be evaluated by direct observation, specific identification, and the interpretation of the effects of local buckling on the members and frameworks of steel-frame structures during a fire. Performance-based design (hereafter, PBD) uses the observed behavior during a real fire for a full range of performance design evaluation, rather than a hypothetical behavior during a fire based on a standard temperature versus heating time curve. Accurate measurement of the conditions of the fire rooms and the structural materials is essential to proper performance evaluation by PBD methods.

In developed countries where performance-based building design is employed, there is definite commitment to enhancing building safety by fire safety assessments, standards, and designs as part of an overall program of national disaster prevention. The two essential goals of PBD design standards and methods are the enhancement of safe and rapid evacuation of occupants, and the minimization of damage and ultimate collapse of an affected building. Domestically, much of the preparation being made for the introduction of PBD methods has come from related fields. Moreover, the developments of the required technology, data base (DB), and personnel are still in their infancy. The purpose of the present study was to investigate the system for evaluating performance during a fire, toward the domestic introduction of the PBD standard. The purpose is to facilitate the construction of buildings with optimal fire safety.

The study was conducted by delimiting the thermal conductivity and mechanical properties within specified prediction ranges. The main objectives of this study were as follows:

- To design an analytic methodology for assessing the resistance of steel members based on the ultimate load and their cross-section size and effective length.
- To determine the steel temperature by heat transfer analysis of the steel section using the standard fire time versus temperature curve.
- To conduct a two-dimensional analysis of thermal-plastic creep in the steel members.
- To evaluate the fire resistance and determine the temperatures at which total failure of the steel members occur.

FIREFLY ALGORITHM TWO-DIMENSIONAL ANALYSIS OF THERMAL CONDITION THROUGH STEEL SECTION

Thermal heat conduction through the steel section was analyzed by finite element analysis using unsteady static heat conduction and the Crank-Nicalson method. The conditions used for the analysis are as follows:

Fire temperature curve: The standard fire time-temperature curve (ISO-834-10: 2014)

Density of steel: 7, 774 (kg/m³)
Convective heat transfer of air: 20 (kcal/m²h°C)

The specific heat of the steel was determined in accordance with a previous work (KICT 2000). In the present study, it was assumed that

$$c = 0.00012 \cdot T + 0.11 \quad @\ 20 \le T \le 600°C \tag{1}$$

$$c = 0.00046 \cdot T - 0.088 \quad @ T > 600°C \tag{2}$$

where T is the temperature of the specimen (°C), and c is the specific heat (kcal/kg°C).

The thermal conduction rate of the steel was also determined using a formula in the same previous work (KICT 2000). In the present study, it was assumed that

$$k = -0.00667 \cdot T + 34 \quad @\ 20 \le T \le 600°C \tag{3}$$

$$k = 0.045 \cdot T + 3.0016 \quad @ T > 600°C \tag{4}$$

where T is the temperature of the specimen (°C), and k is the thermal conduction (kcal/mh°C).

Figure-1 shows the standard time-temperature curve and those obtained in this study for the four faces of the test steel member. The curves suggest a tendency for the temperature to increase with the number of heating surfaces.

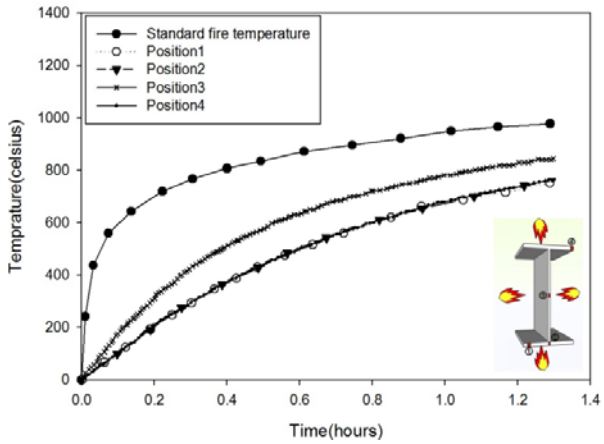

Figure-1. Standard time-temperature curve and those for four sides of test steel member (H-594 × 302 × 12 × 23).

THERMAL ELASTIC-PLASTIC CREEP ANALYSIS

This section describes four models that respectively describe the changes in the elastic modulus, yield stress, creep deformation, and thermal expansion deformation with temperature.

Material models for analysis

Simplification of stress-strain curve

For practical application of a stress-strain curve, the model (Furumura *et al*., 1985) should be simpler than the other expressions used to analyze the mechanical properties of the material. A perfect elastic-plastic model, simplified from the stress-strain curve of SS400 steel which a hysteresis loop observed in elastoplastic materials with isotropic hardening the stress path goes from, is shown in Figure-2. There should be no difference between a perfect elastic-plastic stress curve and a simple stress curve (Furumura *et al*., 1985).

$$\sigma = E \cdot (\varepsilon - p\varepsilon) \tag{5}$$

$$\sigma = 0.01E \cdot normal\ strain + 0.99S_{yRT} - 0.01E \cdot p\varepsilon \tag{6}$$

$$\sigma = 0.01E \cdot normal\ strain + 0.99S_{yRT} - 0.01E \cdot p\varepsilon \tag{7}$$

where σ is the stress (MPa), E is the modulus of elasticity (MPa), ϵ is the strain, S_{yRT} is the yield strength at room temperature (°C), and $p\epsilon$ is the plastic strain.

Modulus of elasticity and yield strength with respect to temperature

The equations of the modulus of elasticity at a given temperature (E_T) and the corresponding yield strength are as follows:

$$E_T / E_{RT} = 1.0 - 0.95 \cdot 10^{-6} \cdot T^2 \tag{8}$$

$$S_{yT} / S_{yRT} = 1.0 - (6.94 \cdot 10^{-7} \cdot T^2) - (5.23 \cdot 10^{-4} \cdot T) \tag{9}$$

where E_T is the modulus of elasticity (MPa) at a given temperature (°C), E_{RT} is the modulus of elasticity (MPa) at room temperature (°C), S_{yT} is the yield strength (MPa) at a given temperature (°C), and S_{yRT} is the yield strength (MPa) at room temperature (°C).

Eqs. (8) and (9) apply to SS400 steel, which is almost identical with mild steel. The presented relationship between the stress and strain under high temperature is based on the results obtained by Furumura *et al*. (1985).

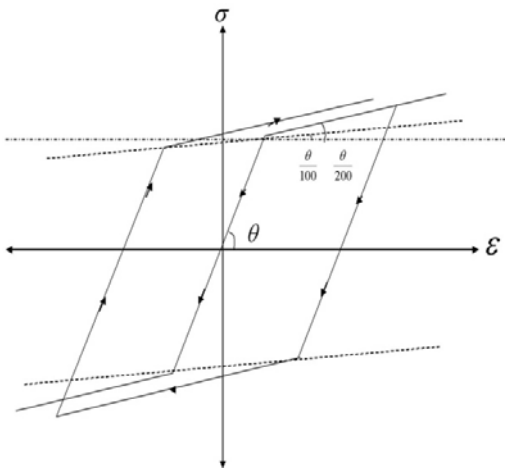

Figure-2. Simple stress-strain curve.

Steel creep properties at high temperature

The creep strain of steel (Okabe and Kohno, 1988) can be calculated using the following equation:

$$\varepsilon_{cr} = 10^{a/T+b} \cdot (\sigma / 9.81)^{c/T+d} \cdot t^{eT+f} \quad (10)$$

where ϵ_{cr} is the creep strain (%), t is the time (minutes), T is the absolute temperature (K), and a–f denote the material number (or material integer). The flow chart of the analysis program for the above conditions is shown in Figure-3.

Table-1. Coefficient for creep strain calculation.

Material No.	Type of steels		
	SS400 (SS41)	**SM490** (SM50)	**SM570** (SM58)
a	-7.212 x 10^3	-8.477 x 10^3	-1.839 x 10^4
b	3.261	4.500	1.710 x 10
c	1.552 x 10^3	3.060 x 10^3	1.035 x 10^4
d	2.249	2.283 x 10^{-1}	-9.586
e	8.984 x 10^{-4}	2.003 x 10^{-3}	2.775 x 10^{-3}
f	-3.3 x 10^{-1}	-1.099	-1.570

PROCEDURE FOR VALIDATING ANALYSIS PROGRAM

Analysis case study I

The above analysis program for the model shown in Figure-4 was experimentally validated. The results of the analysis are shown in Figure-5. The anticipated results of the strain, stress, creep, displacement, and expansion at node number 2 are particularly shown in the figure. As can be observed, the creep strain during the increase of temperature to 250°C rose sharply within 5 min, eventually reaching its peak value in 12 min, whereas there was little change in the creep strain during the period of decreasing temperature. Moreover, the compressive stress due to thermal expansion of the structural steel increased after the temperature had reached 200°C (in about 4 min). There was subsequent gradational decrease in the compressive stress owing to increasing creep strain and deterioration of the materials. When the temperature began to decrease, the cross-sectional stress and total strain also decreased owing to the steel shrinkage phenomenon, and the state of compressive stress was transformed into one of tensile stress.

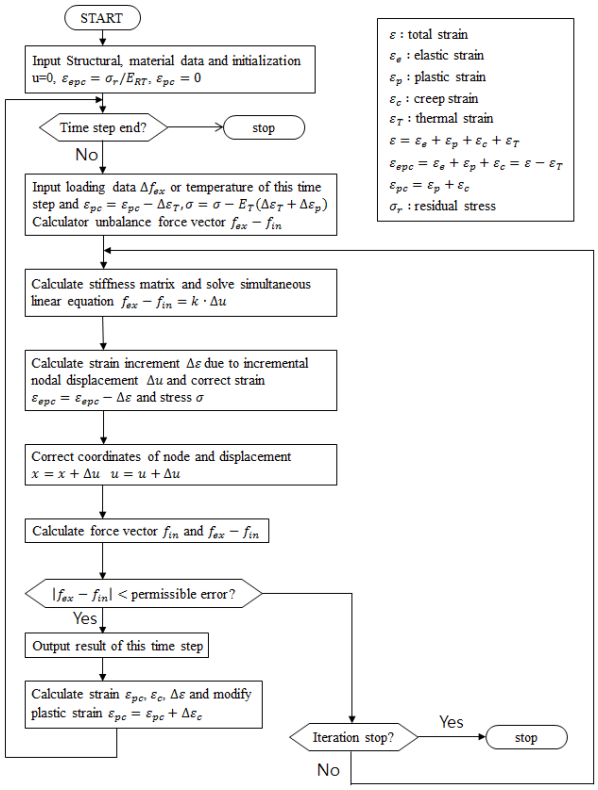

Figure-3. Flowchart of program.

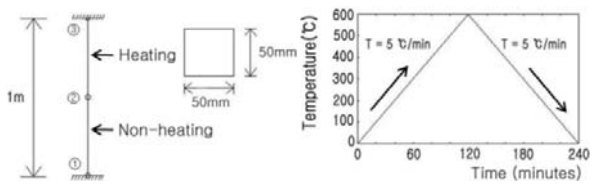

Figure-4. Length, cross section, and temperature versus fire time curve of proposed model.

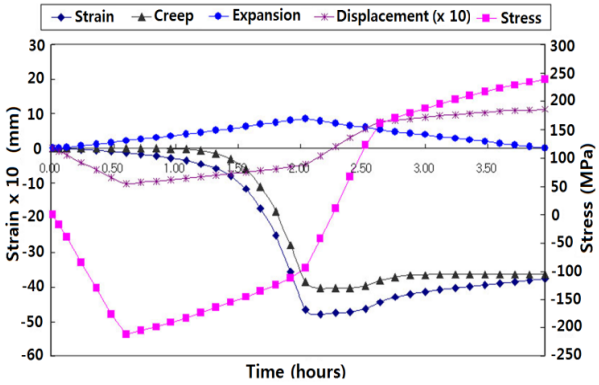

Figure-5. Analysis results of case study I.

Analysis case study II (creep behavior of steel beam in monotype cross section under constant temperature and load)

Furumura *et al.* (1985) conducted a flexural test to determine the deflection of steel over time in a monotype cross section under constant temperature and load. The test progressed satisfactorily from the results of the experimental analysis. The results are shown in Figure-7. The experimental and prediction results are shown in Figure-7, and good agreement can be observed.

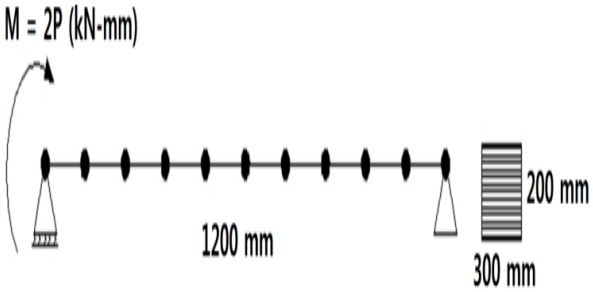

Figure-6. Analysis model of case study II.

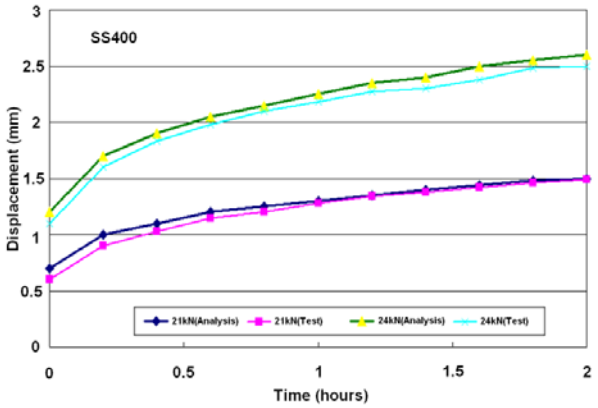

Figure-7. Analysis results of case study II.

Analysis case study III (comparison with maximum deflection of steel with respect to load rate)

The actual maximum deflection of the steel was compared with the results obtained by Cho *et al.* (2003) using the VALCAN program. The maximum bending deflection of the simple beam was determined with respect to the load ratio and compared with the results obtained by VALCAN. The considered load ratios were 0.2, 0.3, 0.4, 0.5, 0.6, and 0.7. The details of the analysis model and the material properties are presented in Figure-8 and Tables 2 and 3.

The maximum bending deflections for different load ratios determined by the present model and the VULCAN program (Cho *et al.*, 2003) are shown in Fig. 9. For load ratios of 0.2–0.4, the maximum displacements predicted by the present model were a little smaller than those determined by the VULCAN program, whereas the former were larger for load ratios of 0.5–0.7. Moreover, the differences were quite small for temperatures above 500°C. Overall, the differences can be attributed to the different material properties and stress-strain curves employed.

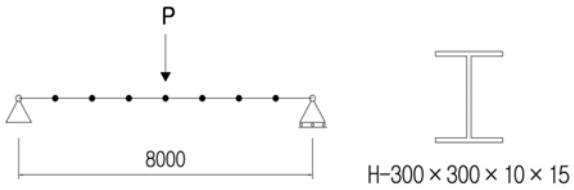

Figure-8. Analysis model of case study III.

Table-2. Material properties of H-300 x 300 x 10 x 15.

Material	**H-section steel**	**Modulus of elasticity**	2.06×10^6 MPa
Yield strength	264.8 MPa	**Number of element divisions**	8

Table-3. Cross section of H-steel and load ratios.

Cross section (mm)	**Central concentrated load** (kN)					
	r					
	0.2	0.3	0.4	0.5	0.6	0.7
H-300x300x10x15	41.3	61.9	82.5	103.1	123.8	144.4

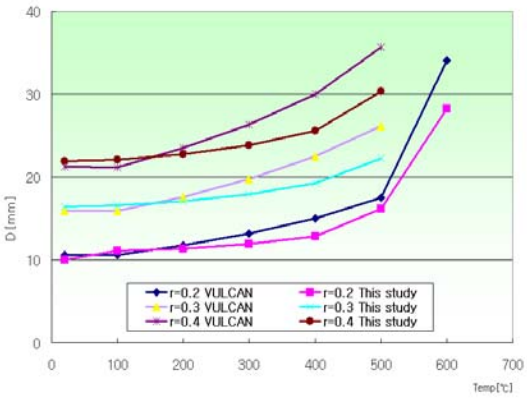

Figure-9. Comparison of maximum displacements determined by present model and Vulcan program for load ratios of 0.2, 0.3, and 0. 4.

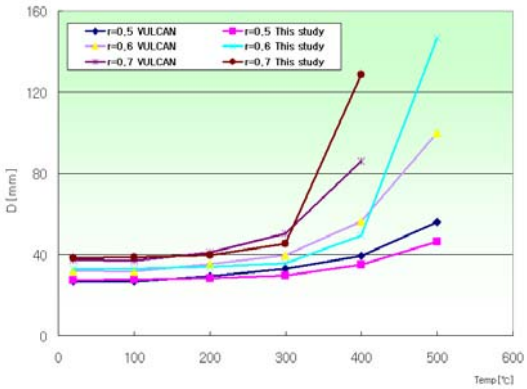

Figure-10. Comparison of maximum displacements obtained by present model and VULCAN program for load ratios of 0.5, 0.6, and 0.7.

ESTIMATION OF FAILURE TEMPERATURE

In the analysis, if the resistance capacity exceeded the ultimate strength, failure of the steel member was considered to occur. At this point, the resistance capacity could be calculated using the following three equations for limit state design (AISC, 2005):

$$N_P = F_Y(T) \cdot A \quad (11)$$

$$M_P = F_Y(T) \cdot Z_P \quad (12)$$

$$V_P = 0.6F_Y(T) \cdot A_W \quad (13)$$

If one of the three equations satisfies "resistance capacity of member > ultimate strength," then

$$M > M_p \quad (14)$$

$$N > N_p \quad (15)$$

$$V > V_p \quad (16)$$

where M is the moment (kN-m), N is the axial force (kN), V is the shear force (kN), M_P is the ultimate moment (kN-m), N_P is the ultimate axial force (kN), V_P is the ultimate shear force (kN), $F_Y(T)$ is the yield strength with respect to the temperature (MPa), Z_p is the plastic section modulus (cm^3), and A_W is the sectional area of the web (cm^2).

If one of equations (14), (15), or (16) is satisfied, the member would evidently have failed. When such failure is determined, the corresponding temperature is the failure temperature at which severe damage to the structure is probable.

MEMBER BEHAVIOR FOR HIGH–TEMPERATURE BOUNDARIES

A review of literature reveals that much study has been conducted on the high-temperature mechanical properties of steel members (Bailey 1995; Cho *et al.* 2003; Li *et al.* 2008; Dwaikat and Kodur 2010). In this aspect of the present study, the mechanical properties of structures such as columns and beams at standard fire temperatures were determined. The failure time, failure temperature, and deformation were also predicted. The results are shown in Figures 13 and 15, where some special notations are used to facilitate understanding. Number *1* indicates "*fixed*" and *0* indicates "*free*". For example, *110* indicates x-axis fixed, y-axis fixed, and moment free. The sizes and conditions of the column and beam used for the analysis are shown in Figures-11 and 12.

In the case of the columns, they were loaded with 3,000 kN while fixed and hinged at either end. There was no significant change on either end at elevated temperatures below the failure temperature, which was 591°C for the fixed end, and 589°C for the hinged end. In the case of the beams, two types of loads were applied, namely, central concentrated loads of 400 and 300 kN, respectively. Three different beams were used, namely, a simple beam, a simple beam fixed at both ends, and a beam simply fixed at one end and with a fixed moment applied via a roller at the other end.

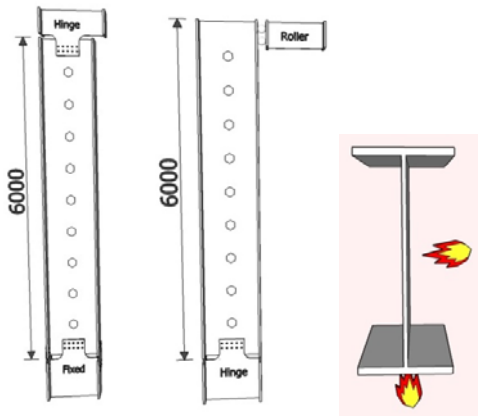

Figure-11. Model of column under high-temperature boundary conditions (unit: mm).

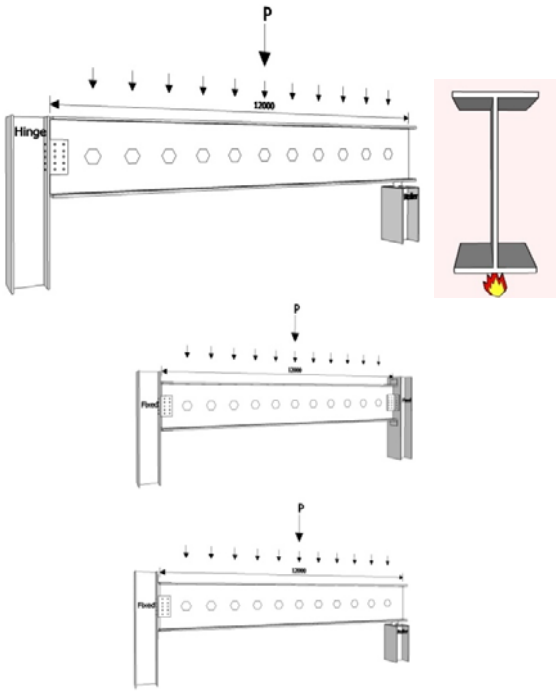

Figure-12. Model of beam under high-temperature boundary conditions (unit: mm).

When the simple beam was heated to 453°C, failure occurred. The simple beam fixed at both ends had the lowest failure temperature, whereas that to which a moment was applied at one end had the highest fire resistance and failure temperature of 630°C. The tested beams are shown in Figure-12, and the deformations of the columns and beams are shown in Figures-14 and 16, respectively. The differences can be attributed to the deformation being significantly dependent on the constraint conditions. The x- and y-axis are shown in Figure-14. A simple beam generally undergoes greater deformation at higher temperatures, and also tends to undergo greater deformation than a simple beam fixed between two columns. Thus, the columns are less affected by the constraint conditions. Conversely, constrained beams undergo greater deformation at higher temperatures. Furthermore, the failure time was affected by the constraints. The column fixed at one end had a failure time of 54 min, whereas that hinged at one end had a failure time of 53 min. The simple beam failed after 83 min, whereas the fixed simple beam and that loaded with a moment failed after 72 and 98 min, respectively.

Table-4. Comparison of failure temperatures and times for different boundary conditions.

Member	**Boundary condition** (BC)	**Failure temperature** (°C)	**Failure time** (min)
Column	111-110	591	54
	110-100	583	53
Beam	110-010	453	83
	111-111	413	72
	111-011	630	98

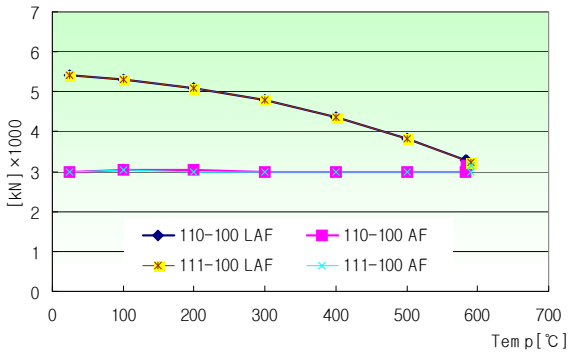

** L.A.F: Full-plastic limit stress (axial force), A.F: Axial force on member, L.E.M: Full-plastic limit stress (moment), B.M: Moment on member*

Figure-13. Comparison of failure temperatures of columns with different boundary conditions.

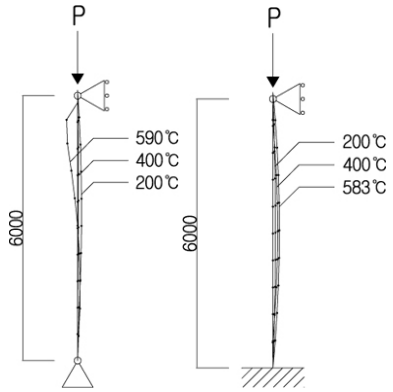

Figure-14. Deformations of columns with different boundary conditions (unit: mm).

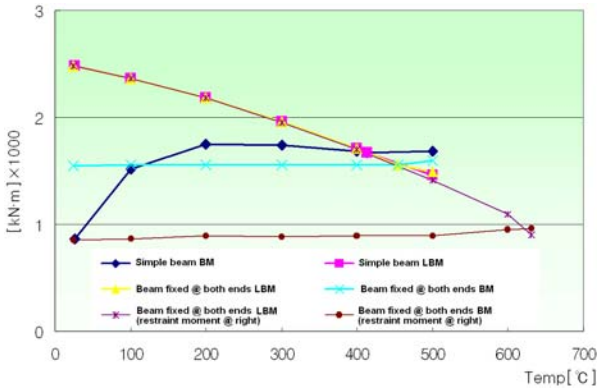

Figure-15. Comparison of failure temperatures of beams with different boundary conditions.

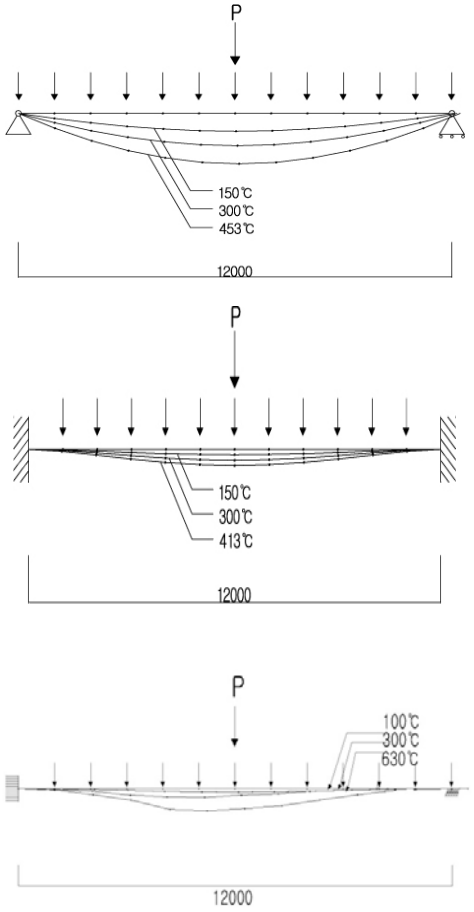

Figure-16. Deformations of beams with different boundary conditions (unit: mm).

CONCLUSIONS

We performed and verified the analyses of the thermal conductivity and thermal-elastic-plastic creep of steel members at high temperatures. Following is a summary of the study and the conclusions drawn regarding the fire behaviors of columns and beams with respect to their boundary conditions.

- The time-temperature data on steel under standard fire temperature conditions obtained by a two-dimensional thermal conductivity analysis using the VALCAN program were in good agreement with those obtained by the presently proposed model of high-intensity heat conduction in a steel member. There was actually minimal difference for temperatures above 500°C.

- The failure time of the members was not significantly affected by the boundary constraint conditions at high temperatures, whereas the failure temperature of the beams was significantly affected. The negative effect on the simple beam was particularly pronounced. The deformation of the constrained columns constitutes a greater disadvantage. The experimentally determined failure times were in very good agreement with those determined by the VALCAN program. In the case of the beams, the failure time of the simple beam tended to be shorter than those of the fixed simple beams, implying lower fire resistance.

- The axis force, shear force, and moment were examined by analyzing the thermal-elastic-plastic creep data of the members, and the temperature distributions were obtained using the standard fire time versus temperature curve. The failure temperatures of the members were determined for computational purposes, beyond the ultimate limit state.

ACKNOWLEDGEMENTS

This study was supported by the research fund of Kumoh National Institute of Technology (2015-104-112).

REFERENCES

AIJ. 1999. Recommendation for Fire Resistance Design of Steel Structures. Architecture Institute of Japan.

AISC. 2005. Steel Construction Manual. 13th edn, American Institute of Steel Construction, Inc., Chicago, IL.

Anderberg Y. 1988. Modelling steel behavior. Fire Safety Journal. 13, pp. 17-26.

Bailey C.G. 1995. Simulation of the structural behaviour of steel-framed buildings in fire. Doctoral Dissertation, University of Sheffield.

Buchanan A.H. 2001. Structural Design for Fire Safety. John Wiley and Sons Ltd, New York, USA.

British Standard International. 1987. Fire Tests on Building Materials and Structures-Part 20: Method for

determination of the fire resistance of elements of construction (general principles). BS 476-20, London.

Cai J. 2002. Developments in modeling of composition building structures in fire. Doctoral Dissertation, University of Sheffield.

Chen J., Young B. and Uy B. 2006. Behavior of high strength structural steel at elevated temperatures. Journal of Structural Engineering, ASCE. 132(12): 1948-1954.

Cho K.-L., Yoon Y.-H. and Kim W.-J. 2003. A study on analysis of thermal stress of steel frame under elevated temperature. Conference Journal of Architectural Institute of Korea. 23(2): 209-212.

Dwaikat M. and Kodur V. 2010. Effect of location of restraint on fire response of steel beams. Fire Technology journal. 46(1): 109-128.

European Code 3 (EC3) 2001. Eurocode 3: Design of Steel Structures-Part 1.2: General Rules-Structural Fire Design. European Committee for Standardization, DD ENV 1993-1-2: 2001, CEN, Brussels.

Furumura F., Ave T., Okabe T. and Kim W. J. 1985. A uniaxial stress-strain formula of structural steel at high temperature and its application to thermal deformation analysis of steel frames. Journal of Structural and Construction Engineering, Trans. of A.I.J. 363, pp. 92-100.

ISO. 2014. Fire Resistance Tests-Elements of Building Construction. ISO-834, Geneva.

Japan Building Center. 1989. Comprehensive Fire Protection Design Method–Fire Resistance Design. 4, p. 39.

JBC. 1998. Limit State Design of Steel Structures Guideline. Japan Institute of Building Construction, Tokyo.

JSSC. 1973. A Study on Standard Live Fire Load for Application to Design in a Building. Japanese Society of Steel Construction.

KICT. 2000. A Research on Updating Standard for Fire Design. Korea Institute of Construction Technology.

KICT. 2000. Establishment of Fire Safety System in Building: Improvement of Building Fire Safety Regulations. Korea Institute of Construction Technology.

KICT. 2001. Establishment of Fire Safety System in Building: Fire Resistance Design Database in Building. Korea Institute of Construction Technology.

KBC. 2009. Korean Steel Structure Design Code - Load and Resistant Factored Design. Ministry of Land, Transport and Maritime Affairs.

Kirby B. R. and Preston R. R. 1988. High temperature properties of hot-rolled, structural steels for use in fire engineering design studies. Fire Safety Journal. 13, 27-37.

Kodur V., Dwaikat M. and Fike R. 2010. High-temperature properties of steel for fire resistance modeling of structures. Journal of Materials in Civil Engineering, ASCE. 22(5): 423-434.

Li G.-Q. and Guo S. X. 2008. Experiment on restrained steel beams subjected to heating and cooling. Journal of Constructional Steel Research. 64(3): 268-274.

Nippon Steel Corporation (NKK) 1988. Fire-Resistant Steel for Building Structural Use, Cat. No. EXE 381, Nippon Steel Corporation, Tokyo.

Poh K.W. 2001. Stress-strain-temperature relationship for structural steel. Journal of Materials in Civil Engineering, ASCE. 13(5): pp. 371-379.